Chemical Physics 504 (2018) 66–71

Contents lists available at ScienceDirect

Chemical Physics

journal homepage: www.elsevier.com/locate/chemphys

First-principles investigation on the mechanism of photocatalytic properties for cubic and orthorhombic $KNbO_3$

Yong-Qiang Xu [a,b,*], Shao-Yi Wu [a,*], Chang-Chun Ding [a], Li-Na Wu [a], Gao-Jun Zhang [a]

[a] *Department of Applied Physics, School of Physics, University of Electronic Science and Technology of China, Chengdu 610054, PR China*
[b] *College of Physics and Electronic Information, Gannan Normal University, Ganzhou 341000, PR China*

ARTICLE INFO

Article history:
Received 11 December 2017
In final form 4 March 2018
Available online 5 March 2018

Keywords:
Photocatalytic properties
Electronic structures
Optical absorption spectra
Cubic andorthorhombic $KNbO_3$

ABSTRACT

The geometric structures, band structures, density of states and optical absorption spectra are studied for cubic and orthorhombic $KNbO_3$ (C- and O-KNO) crystals by using first-principles calculations. Based on the above calculation results, the mechanisms of photocatalytic properties for both crystals are further theoretically investigated to deepen the understandings of their photocatalytic activity from the electronic level. Calculations for the effective masses of electron and hole are carried out to make comparison in photocatalytic performance between cubic and orthorhombic phases. Optical absorption in cubic phase is found to be stronger than that in orthorhombic phase. C-KNO has smaller electron effective mass, higher mobility of photogenerated electrons, lower electron-hole recombination rate and better light absorption capacity than O-KNO. So, the photocatalytic activity of cubic phase can be higher than orthorhombic one. The present work may be beneficial to explore the series of perovskite photocatalysts.

1. Introduction

In order to solve the increasing environmental pollution and future energy crisis brought on by a mismatch between growth in supply and greater growth in demand, photocatalysts have attracted more and more interest due to their potential applications in environmental purification and fuel production in recent years [1–4]. Since Fujishima and Honda [5] reported catalytic water splitting for hydrogen generation on semiconductor electrode composed of titanium dioxide (TiO_2) in 1972, an increasing number of investigations have been performed on semiconductor-based photocatalysts such as TiO_2, ZnO, $NaNbO_3$, $KNbO_3$, $SrTiO_3$, $NaTaO_3$ and $KTaO_3$, etc [5–11]. Among various semiconductor photocatalysts, potassium niobate ($KNbO_3$) has been proved to be suitable for photocatalytic water splitting for hydrogen generation under ultraviolet (UV) light irradiation [12,13] due to long term durability, wide availability, non-toxicity and cost-effectiveness. $KNbO_3$ (KNO) has mainly four different crystalline phases, namely, cubic, tetragonal, orthorhombic and rhombohedral [14]. At high temperatures (>710 K), KNO crystallizes in cubic paraelectric phase (space group $Pm\bar{3}m$), while it shows orthorhombic symmetry (space group Bmm2) at ambient temperature [15].

Generally, many photocatalysts have polymorphs, and their photocatalytic performances usually depend strongly on respective crystal structures and phases, as reported for many different semiconductor photocatalysts [10,12,13,16–22]. Among them, the popular photocatalyst TiO_2, anatase is found to display much higher photocatalytic activity than both rutile and brookite [16–19]. Ye et al. [20] studied the photocatalytic activity of the two phases of perovskite $NaNbO_3$, and the rate of H_2 evolution on cubic $NaNbO_3$ was found to be nearly twice that on the orthorhombic phase. Liu et al. [10,22] performed intensive investigations on the photocatalytic efficiency of pristine and La-doped monoclinic (or cubic) and orthorhombic $NaTaO_3$ (here the cubic phase was adopted to simulate the monoclinic phase due to their similar structures and less expensive calculations). The possible reason why monoclinic (or cubic) phase of $NaTaO_3$ has higher photocatalytic efficiency than orthorhombic phase was systematically analyzed using first-principles methods. These researches gave important inspiration to the present work, which may be regarded as a parallel study as that of Refs. [10,22] to some extent. Recent experimental study on the photocatalytic water splitting for hydrogen generation on KNO submicro-crystals under UV irradiation [13] revealed that the surface area-normalized rate of H_2 production over submicro-cubes with cubic phase is twice larger than that on orthorhombic one. However, to the best of our knowledge, theoretically, the major factors affecting the photoactivity differences between cubic

---

* Corresponding authors at: Department of Applied Physics, School of Physics, University of Electronic Science and Technology of China, Chengdu 610054, PR China (Y.Q. Xu).

E-mail addresses: yqxu666@163.com (Y.-Q. Xu), wushaoyi@uestc.edu.cn (S.-Y. Wu).

https://doi.org/10.1016/j.chemphys.2018.03.007

and orthorhombic $KNbO_3$ (C- and O-KNO) crystals have not been sufficiently clarified so far. Neither has the synthetical theoretical investigation on the detailed physical mechanism of photocatalytic properties been performed for both polymorphs. Especially, the following interesting issues are worthy of further investigations. (1) In view of the comparable band gaps of C- and O-KNO crystals based on the previous experimental results [12,13], why can produce huge difference in the photocatalytic activity between the two systems? (2) As presented in Ref. [10] by Liu et al., the effective masses of carriers play an important role in transfer, separation and mobility of photo-generated electrons and holes and hence in photocatalytic activity. So the detailed investigation on the effective masses of carriers can be helpful to understand the differences in photocatalytic performances between C- and O-KNO. Unfortunately, the related study on the effective masses of carriers for both polymorphs is rather scarce until now. (3) Characteristic of the optical absorption spectra can reflect the photcatalytic performance of a photocatalyst. However, to our knowledge, no comparison research has been reported on the absorption coefficient for both polymorphs. So the differences in light absorption capacity between C- and O-KNO are worthy to be further studied.

To answer and understand the above issues, the comparative investigation is employed in this work on the crystal structures, band structures, density of states, optical absorption spectra and the effective masses of photo-generated electrons and holes of C- and O-KNO crystals in the frame of first-principles density functional theory (DFT) to provide a theoretical understanding of the differences in photocatalytic performance between both polymorphs. The outline of this paper is as follows. In section 2, the computational details of present work are illustrated. In section 3, the differences in photocatalytic performance between C- and O-KNO crystals are illustrated and discussed. Finally, the conclusion is drawn in section 4. Present work would deepen the understanding of the photocatalytic mechanism for both crystals from the electronic level.

2. Computational details

All the first-principles DFT calculations are performed using the Vienna ab initio Simulation Package (VASP) [23–25]. The optimizations of both polymorphs are carried out using the generalized gradient approximation (GGA) with Perdew-Burke-Ernzerhof (PBE) functional [26] and hybrid function HSE06 [27] for comparison. The projector augmented wave potentials [28] are used to describe the interaction between the ionic core and valence electrons. The valence electrons taken into account for KNO are $3s^23p^64s^1$ for K, $4p^64d^45s^1$ for Nb and $2s^22p^4$ for O, respectively, with the rest of electrons frozen as core states. The cutoff energy of 500 eV is used. The convergence threshold for self-consistent field iteration is set as 10^{-6} eV. The lattice parameters and atomic coordinates are relaxed until the forces on each atom are below 1 meV/Å. The Brillouin-zone integrations are performed using a shifted Monkhorst-Pack $7 \times 7 \times 7$ and $7 \times 11 \times 7$ k-point mesh for cubic and orthorhombic phases, respectively. To obtain reliable electronic structures and optical absorption spectra, the hybrid function HSE06 [27] scheme is adopted to calculate the above properties. For the sake of ensuring the accuracy of present computations, the higher cutoff energy and bigger k-points are also adopted, whereas the results indicate almost no variation in the energy and geometric structures for both polymorphs.

3. Results and discussion

3.1. Crystal structures

The conventional unit cell of C- and O-KNO crystals are presented in Fig. 1 with VESTA software package [29]. Optimizations of the geometric structures are performed with PBE and HSE06 schemes before the computations of the electronic structures. The optimized lattice parameters are $a = 4.057$ Å for C-KNO and $a = 5.823$ Å, $b = 4.016$ Å, $c = 5.860$ Å for O-KNO with PBE, and $a = 4.014$ Å for C-KNO and $a = 5.719$ Å, $b = 3.972$ Å, $c = 5.748$ Å for O-KNO with HSE06, respectively. From the experimental values ($a = 4.011$ Å [30] for C-KNO and $a = 5.695$ Å, $b = 3.973$ Å, $c = 5.721$ Å [14] for O-KNO), the optimized results with no more than 2.5% errors by using HSE06 are better, suggesting that the pseudopotential adopted is appropriate for the present calculations.

3.2. Electronic structures

To examine the origin of the discrepancy in photocatalytic performances between C- and O-KNO crystals, the band structures and partial density of states (PDOS) are calculated with hybrid function HSE06 scheme and shown in Fig. 2, which reveals distinct band structures for the two systems. Comparing the profile of band along high symmetry directions, particularly at the edge of conduction band, one can see that all states of the conduction band in C-KNO exhibit strong dispersion except that along Γ-X path is relatively flatter. Particularly, in the vicinity of Γ and X high symmetry points, it is very dispersive along R-X-M and R-Γ-M paths. Although the dispersion is also found along Γ-Z, Z-T-Y and S-X-U paths for O-KNO in Fig. 2(b), the degree of dispersion in the orthorhombic phase is less than in the cubic one, implying smaller electron effective masses and higher electron mobility in the latter. The related properties are to be discussed in detail in the following subsection. According to PDOS, present conduction band and valence band are dominantly composed of O_2p and Nb_4d states with obvious hybridization, reflecting the covalent nature of the Nb-O bonds. Unlikely, absence of hybridization between K and Nb or O electronic states reveals ionic interaction between K and NbO_6 octahedral group. Since the top of valence band and the bottom of conduction band arise mainly from O_2p and Nb_4d states, respectively, for both C- and O-KNO, photoelectrons largely transfer from O_2p to Nb_4d orbitals in both systems, and the transitions between the two states may strongly affect the photocatalytic activity of the systems.

From Fig. 2(a) and (b), the density of energy band of O-KNO is higher than C-KNO. The possible reasons may be illustrated as follows. First, there are actually two units of KNO in the orthorhombic phase unit cell while only one unit in the cubic phase unit cell. So it is natural that these two units will yield more electronic bands. Second, according to the crystal field theory [31], the constitutions of the electronic structures are closely relevant to Nb_4d orbital splittings under the cubic and orthorhombic oxygen octahedral crystal fields in C- and O-KNO, respectively. The cubic octahedral crystal field leads to a splitting of the five-fold degenerated Nb_4d orbitals into a lower triply degenerated t_{2g} orbitals (d_{xy}, d_{yz}, d_{zx}) and a higher doubly degenerated e_g orbitals ($d_{x^2-y^2}$, d_{z^2}) in C-KNO. As regards O-KNO, the degeneracy of both t_{2g} and e_g sublevels can be further removed due to the orthorhombic distortion. Therefore, the denser band distributions of O-KNO than C-KNO can be understood.

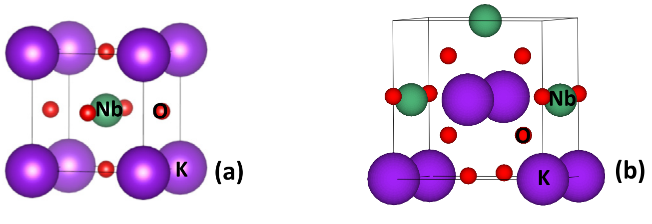

Fig. 1. The unit cell of cubic (a) and orthorhombic (b) KNO.